
AN ACCURACY ANALYSIS OF SMALL ANGLE MEASUREMENT USING THE OPTICAL VORTEX INTERFEROMETER

Ewa Frączek, Janusz Mroczka

Wrocław University of Technology, Chair of Electronic and Photonic Metrology, B. Prusa 53/55, 50-317 Wrocław, Poland
(✉ ewa.fraczek@pwr.wroc.pl, +71 320 6329, janusz.mroczka@pwr.wroc.pl)

Abstract

In recent years a lot of effort has been put into testing and improving the idea of a three-beam interferometer known as Optical Vortex Interferometer (OVI). Devices based on the idea of an OVI allow, among other things, measuring small rotation angles of the wave [1]. In this paper complex statistical analysis has been used for the results of the small-angle rotation wave measuring method. The authors of this paper claim that the presented analysis of data handling error in a new measurement method increases the accuracy of the measured angle by better choice of random triplets.

Keywords: optical vortex, small angle measurements, interferometry.

© 2009 Polish Academy of Sciences. All rights reserved

1. Introduction

Optical interferometry is one of the most interesting domains of optical measurement techniques. In this paper a new kind of interferometer – Optical Vortex Interferometer (OVI), is discussed. In the OVI three plane beams interfere to generate the regular lattice of Optical Vortex (OVs) [2]. The optical vortex (OV) is an isolated central point where the phase is undetermined and the intensity is zero – the OV is an example of interesting and unique type of such a marker. The OVs are more and more frequently used in new applications [3-7]. One of them is the Optical Vortex Interferometer used for the measurement of small angles of rotation [1,8]. To perform a single measurement, the method described in [9,10] requires four separate interferograms (A+B, A+C, B+C, A+B+C). One wave, for example C, can be deflected by a wedge, so the wavevector of the C wave is rotated. When one wave is deflected, the optical vortices change the position. All information about the object is obtained from the relative position of the vortex points in the regular lattice. In the past, other authors [8] used basic statistic methods to analyze the obtained results. This paper shows that the statistical analysis can be more precise. In the next section more information on the numerical algorithm for the small-angle rotation measurement will be presented.

2. The numerical algorithm

Jan Masajada [1] shows the idea of small-angle rotation measurement. In this paper we will show only the necessary steps to explain the need for the change of the statistical analysis.

The optical wedge, put in one of the arms of the OVI, changes the coordinates of the wavevector k_C of the size Δk_{x_C} and Δk_{y_C} [1]. Application of the Optical Vortex Interferometer to the measurement enables calculation of the components Δk_{x_C} and Δk_{y_C} from the following equations

$$\Delta k_{x_C} = \frac{(\Delta x_2 \cdot \Delta y_{n1} + \Delta x_{n1} \cdot \Delta y_{n2} - \Delta x_1 \cdot \Delta y_{n2} - \Delta x_{n2} \cdot \Delta y_{n1}) \cdot k_{x_{BC}}}{\Delta x_{n1} \cdot \Delta y_{n2} - \Delta y_{n1} \cdot \Delta x_{n2}} + \frac{(\Delta y_2 \cdot \Delta y_{n1} - \Delta y_1 \cdot \Delta y_{n2}) \cdot k_{y_{BC}}}{\Delta x_{n1} \cdot \Delta y_{n2} - \Delta y_{n1} \cdot \Delta x_{n2}} \quad (1a)$$

$$\Delta k_{y_C} = \frac{(\Delta y_1 \cdot \Delta x_{n2} + \Delta x_{n1} \cdot \Delta y_{n2} - \Delta y_2 \cdot \Delta x_{n1} - \Delta y_{n1} \cdot \Delta x_{n2}) \cdot k_{y_{BC}}}{\Delta x_{n1} \cdot \Delta y_{n2} - \Delta y_{n1} \cdot \Delta x_{n2}} + \frac{(\Delta x_1 \cdot \Delta x_{n2} - \Delta x_2 \cdot \Delta x_{n1}) \cdot k_{x_{BC}}}{\Delta x_{n1} \cdot \Delta y_{n2} - \Delta y_{n1} \cdot \Delta x_{n2}} \quad (1b)$$

To calculate the rotation angle, one needs to consider the relative position of the three vortex points. Fig. 1 shows two exemplary random triplets P1, P2, P3 and Pn1, Pn2, Pn3 taken for the calculation. Δx_1 and Δy_1 are the differences in x and y coordinates between P2 and P1 before the rotation (Δx_{n1} , Δy_{n1} are – the differences in x and y coordinates between Pn2 and Pn1 after the rotation). Similarly, Δx_2 and Δy_2 are the differences in x and y coordinates between P3 and P1 before the rotation (Δx_{n2} , Δy_{n2} - the differences in x and y coordinates between Pn2 and Pn1 after the rotation).

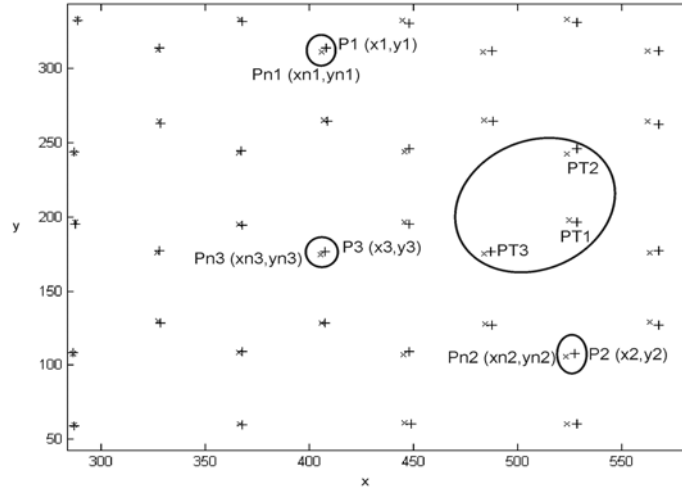


Fig. 1. The position of the vortex points as measured without the wedge (marker “+”) and with the wedge (marker “x”). PT1, PT2, PT3 determine the small triplet. Points P1, P2, P3 and Pn1, Pn2, Pn3 create random triplets.

The wavevector \mathbf{k}_{BC} ($k_{x_{BC}}$, $k_{y_{BC}}$) is defined in the following way

$$k_{x_{BC}} = k_{x_B} - k_{x_C}, \quad (2a)$$

$$k_{y_{BC}} = k_{y_B} - k_{y_C}, \quad (2b)$$

These values ($k_{x_{BC}}$, $k_{y_{BC}}$) can be calculated from the following formulas

$$k_{x_{BC}} = \frac{\Delta y_1 \cdot \Delta \varphi_{13} - \Delta y_2 \cdot \Delta \varphi_{12}}{\Delta x_2 \cdot \Delta y_1 - \Delta y_2 \cdot \Delta x_1}, \quad (3a)$$

$$k_{y_{BC}} = \frac{\Delta x_2 \cdot \Delta \varphi_{12} - \Delta x_1 \cdot \Delta \varphi_{13}}{\Delta x_2 \cdot \Delta y_1 - \Delta y_2 \cdot \Delta x_1}, \quad (3b)$$

In this case the author [1] uses the geometry of the vortex points lattice. In this method the small vortex triplet (PT1, PT2, PT3 in Fig. 1) must be created from three nearest neighbouring

points. The phase difference $\Delta\varphi$ between waves B and C changes by $\Delta\varphi_{13} = \frac{2}{3}\pi$ (while moving from point PT1 to PT3) and while moving from point PT1 to PT2 by to $\Delta\varphi_{12} = \frac{2}{3}\pi$.

The symbols $\Delta x_1, \Delta x_2, \Delta y_1, \Delta y_2$ are the distances measured along the axes x and y between points PT2 and PT1 ($\Delta x_1, \Delta y_1$) and PT3 and PT1 ($\Delta x_2, \Delta y_2$).

In the described algorithm, at first, the coordinates of the wavevector kC are calculated from all possible small triplets. Each small triplet contains three vortex points with the same geometrical configuration. Usually in a measurement it is possible to determine a few hundred small triplets in the analysed area. Then, step the mean value and the standard deviation is calculated. Due to huge number of choosing three points from more than a thousand only from a few thousand random triplets the values Δk_{xC} and Δk_{yC} (1) are evaluated. Not all possible vortex triplets are equally suitable for the calculations. For each accepted triplet the following condition must be fulfilled [1]

$$form1 = |\Delta x_{n1} \cdot \Delta y_{n2} - \Delta y_{n1} \cdot \Delta x_{n2}| \text{ or } form2 = |\Delta y_1 \cdot \Delta x_{n2} - \Delta x_{n1} \cdot \Delta y_2|. \quad (4)$$

Parameters *form1* and *form2* should be greater than a critical value (e.g. 2). The value is different for different experimental data. If these parameters are smaller than the value, the calculations will result errors or the distribution of the refracting angel of the wedge will not be symmetrical. This problem will be discussed further on.

The described method can be used to determine the refracting angle γ of the wedge. When the wedge is rotated only around the axis x, the angel γ can be obtained from the following formula

$$\gamma = \arctan \left(\frac{\sin \left(\frac{\Delta k_{xC}}{k} \right)}{n - \cos \left(\frac{\Delta k_{xC}}{k} \right)} \right), \quad (5)$$

where $k = \frac{2\pi}{\lambda}$, $\lambda = 632,8 \text{ nm}$, $n = 1,515$.

3. Analysis of the statistical error

The problem with nonsymmetrical distribution of the refracting angel of the wedge was tested numerically. Firstly, perfect interferograms with one wave rotation were generated. The refracting angle of the wedge was calculated and the distribution of this angle was analysed. Secondly the imperfect interferograms were generated. Noise was added in the simulation. The parameters of the noise where determined appropriately to the experimental conditions. A lot of cases with different values of parameter *form* (4) were analysed. Exemplary results for the perfect end with noisy case below are presented.

The parameter *form1* or *form2* (4) eliminates one kind of the triplets. Those triplets are created by collinear points. In Fig. 2 we can see a change in the calculated histograms of the wedge refracting angle with the use of different limits of the parameter *form1* (for *form 2* we can see the same histograms). In the numerical calculation 6000 random triplets have been chosen. For example, for the parameter *form 1* >1 we have about 4450 triplets (for the *form 1* >3 we have about 2400 triplets, for the *form 1* >5 we have about 1050 triplets). The analysis of the histograms shows lack of symmetry in the distribution of the wedge refracting angle, so

the mean value and the standard deviation are bad parameters to specify this distribution. It is not a Gaussian distribution. The authors searched other parameters to reject inconvenient triplets.

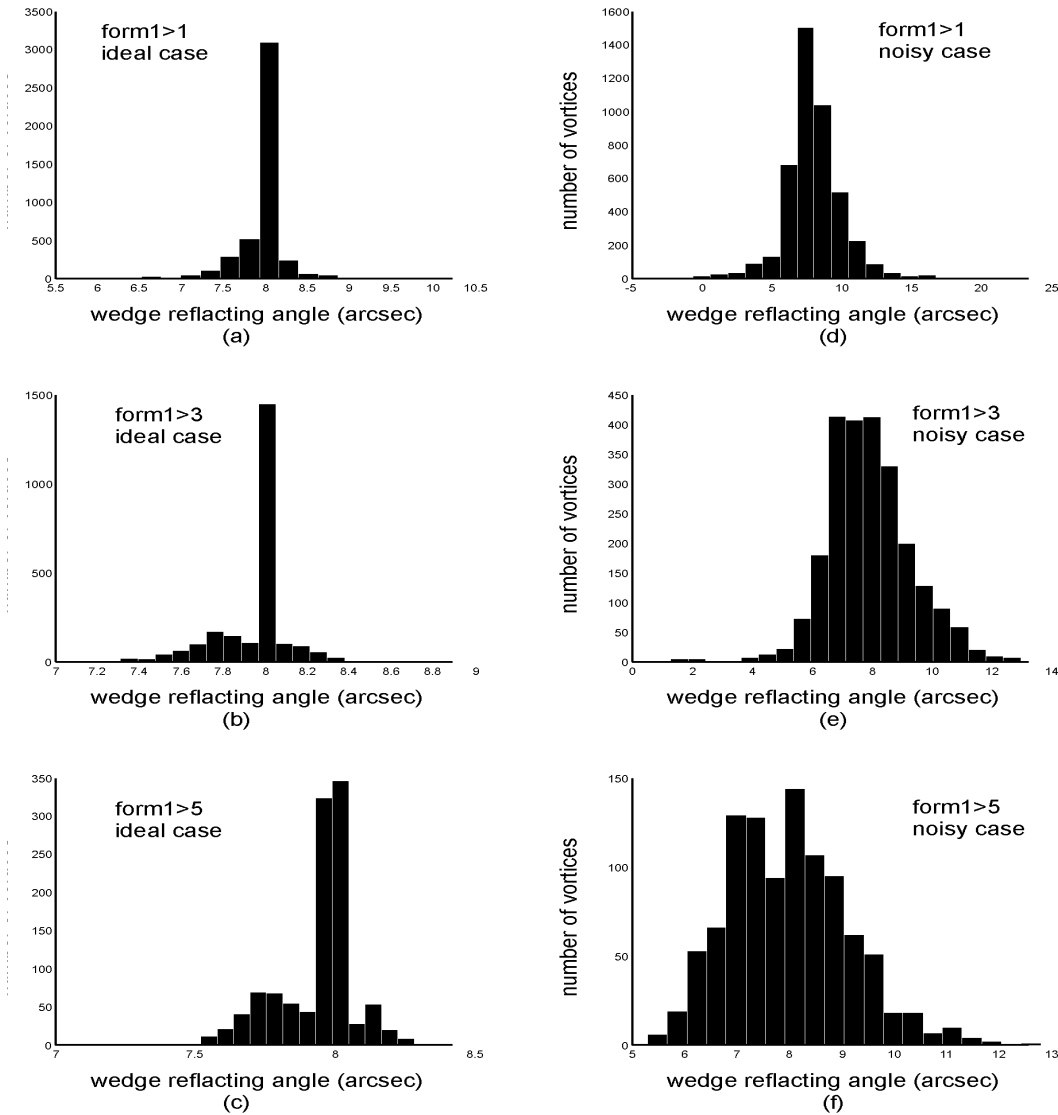


Fig. 2. Calculated histogram of the wedge reflecting angle from the numerical interferograms: (a), (b), (c) - the ideal case, (d), (e), (f) - the noisy case; (a) and (d) - the parameter form1>1, (b) and (e) - the parameter form1>3, (c) and (f) - the parameter form1>5. The value of the calculated wedge refracting angle is 8 arcsec.

We tested three parameters T, F and H. The results of exemplary calculation for those parameters are presented below.

3.1 The parameter T

With the aim of determining the first parameter T, a simple rule was used. It's a well-known fact that the sum of any two segments of a triangle is bigger than the third one. In the numerical test we used the following form

$$a + b > c \cdot T \quad \text{and} \quad b + c > a \cdot T \quad \text{and} \quad a + c > b \cdot T \quad (6)$$

where a, b, c are the sides of the triangle, T is a parameter. The value of T changes from 1.01

to 1.30. Fig. 3 shows histograms of the wedge refracting angle calculated from the numerical interferograms.

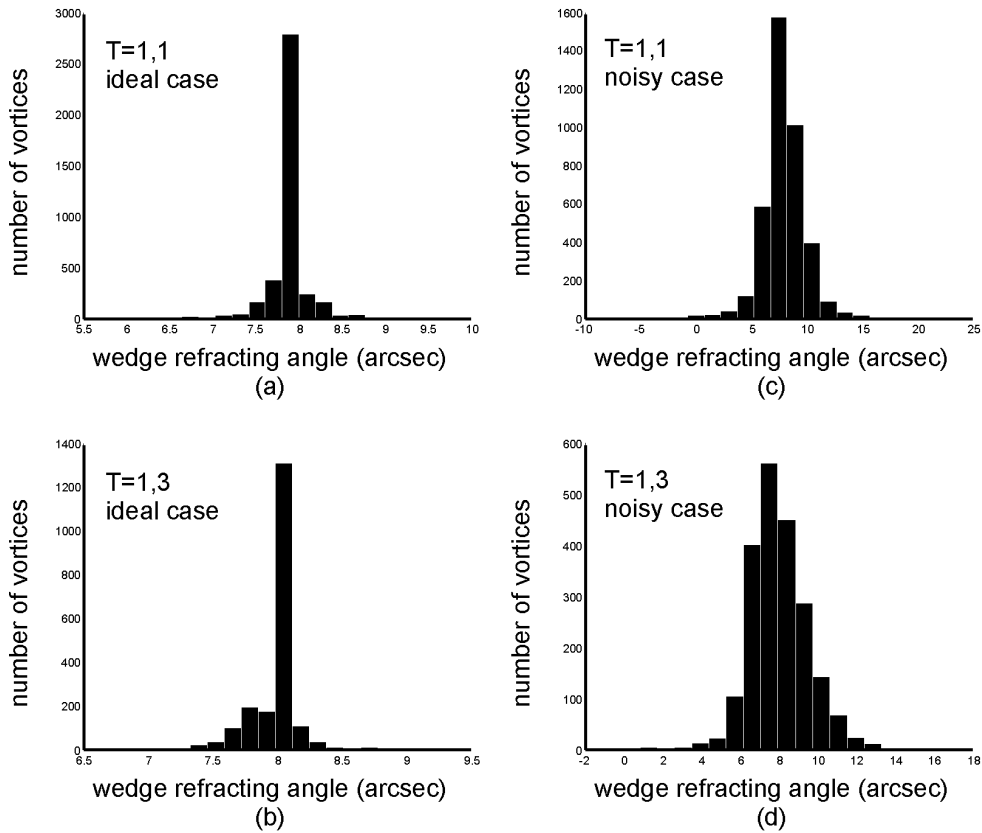


Fig. 3. Calculated histogram of the wedge refracting angle from the numerical interferograms: (a), (b) - the ideal case, (c), (d) - the noisy case; (a) and (c) - the parameter $T=1.10$, (b) and (d) - the parameter $T=1.30$. The value of the calculated wedge refracting angle is 8 arcsec.

The analysis of the results of the numerical test shows that the parameter T has to occur between 1.01 and 1.20. When the value of the parameter T is bigger than 1.20 then the distribution of the wedge refracting angle is nonsymmetrical. Fig. 3 shows selected histograms presenting the results of exemplary calculation for the perfect and noisy case, respectively.

3.2 The parameter F

The parameter F corresponds to the value of the field of the triangle made from three triplet points. The triangles with an insufficient value of the field were not considered for further calculation. In the numerical tests we applied the following formula

$$\text{Field}_{\max} \cdot F < \text{Field}_n, \quad (7)$$

where $n=1,2,\dots,6000$ triplets, the value of F changes from 0.01 to 0.40.

Change of value of the parameter F affects the symmetry of histogram. Only for the parameter F included between 0.01 and 0.10 the symmetry of histograms is maintained. The results of the exemplary calculation for those parameters are presented below.

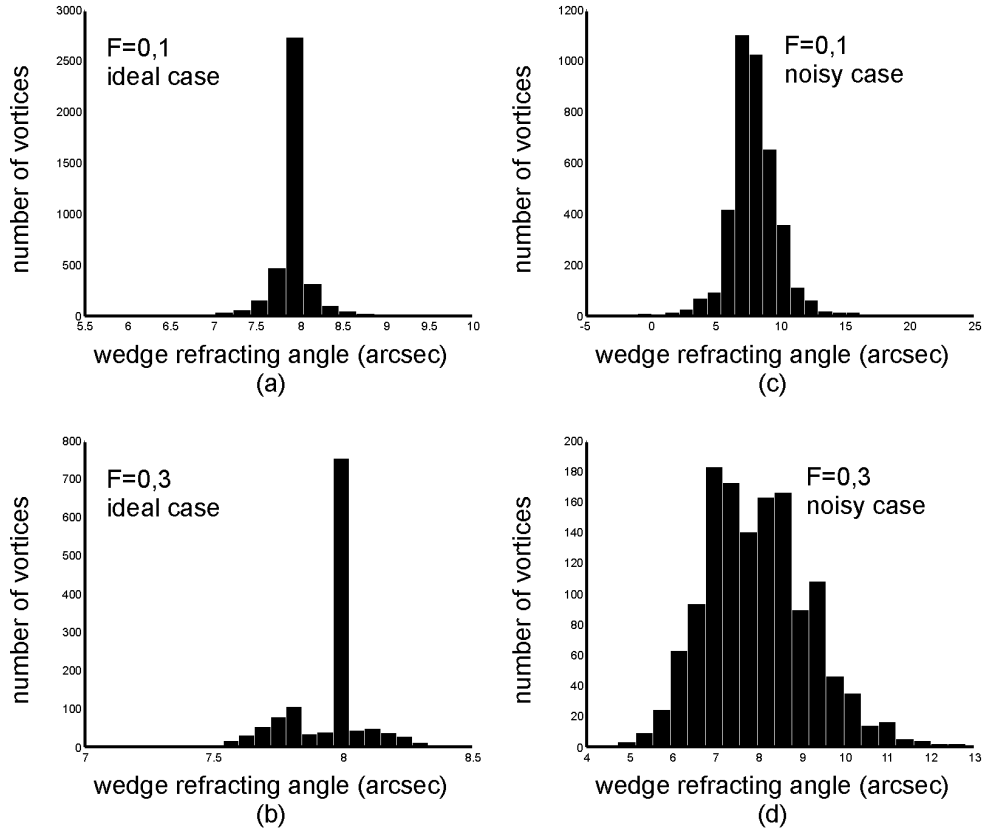


Fig. 4. Calculated histogram of the wedge refracting angle from the numerical interferograms: (a), (b) - the ideal case, (c), (d) - the noisy case; (a) and (c) - the parameter $F=0.10$, (b) and (d) - the parameter $F=0.30$. The value of the calculated wedge refracting angle is 8 arcsec.

3.3 The parameter H

The parameter H determines the value of the triangle height created by three random vortex points. In the numerical test we use the following form

$$h_a > h_{a_{\max}} \cdot H \quad \text{and} \quad h_b > h_{b_{\max}} \cdot H \quad \text{and} \quad h_c > h_{c_{\max}} \cdot H, \quad (8)$$

where, the value of H changes from 0.01 to 0.40.

Fig. 5 shows selected histograms of the calculated wedge refracting angle values from the numerical interferograms. Every change in value of the discussed parameter affects the symmetry of distribution of the wedge refracting angle.

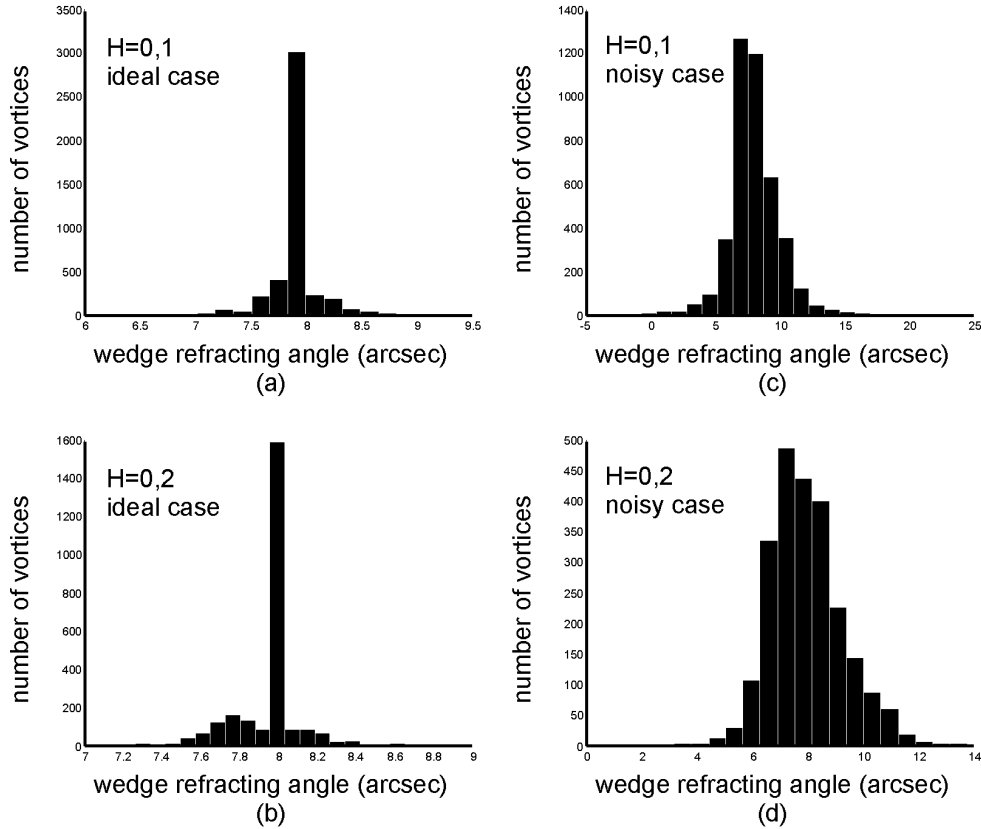


Fig. 5. Calculated histogram of the wedge refracting angle from the numerical interferograms: (a), (b) - the ideal case, (c), (d) - the noisy case; (a) and (c) - the parameter $H=0,10$, (b) and (d) - the parameter $H=0,20$. The value of the calculated wedge refracting angle is 8 arcsec.

4. The experiment

The last step was to apply the procedure described above to the interferograms obtained from the experiment. The mean value of the wedge reflecting angle measured with the auto collimation method was 6 ± 2 arcsec. We used different parameters, described above, for the calculation. Symmetric distribution for the probability density function was observed for the following parameters: $T \in \langle 1.05, 1.20 \rangle$ and $F \in \langle 0.05, 0.20 \rangle$. Then the mean value μ and standard deviation σ^2 were calculated from the experimental data. Fig. 6a shows the Gaussian distribution (solid line) plotted from those calculation parameters μ and σ^2 . Fig. 6b we can see another diagram (solid line) with modified parameters of the Gaussian distribution. The standard deviation in the second diagram (Fig. 6b) is smaller than the standard deviation in the first graph of the Gaussian distribution. The parameters of the normal distribution automatically calculated from the experimental data describe the real situation inaccurately.

The Cauchy-Lorentz distribution described the experimental data better than the Gaussian distribution. Two parameters were used for describing the Cauchy-Lorentz distribution: x_0 is the location parameter specifying the location of the peak of the distribution, and γ is the scale parameter specifying the half-width at half-maximum. Fig. 6 shows the Cauchy-Lorentz distribution (broken line) plotted from the experimental data. The results of measurement parameters of the wedge refracting angle with the Optical Vortices Interferometer should be described by the parameters of the Cauchy-Lorentz distribution. Instead of the mean value, the modal value was used. For the experimental data the mean value and the modal value are the same. In case when the obtained distribution was nonsymmetrical the mean value was

incorrect. In this case the modal value should be used to determine the value of the tested object angle.

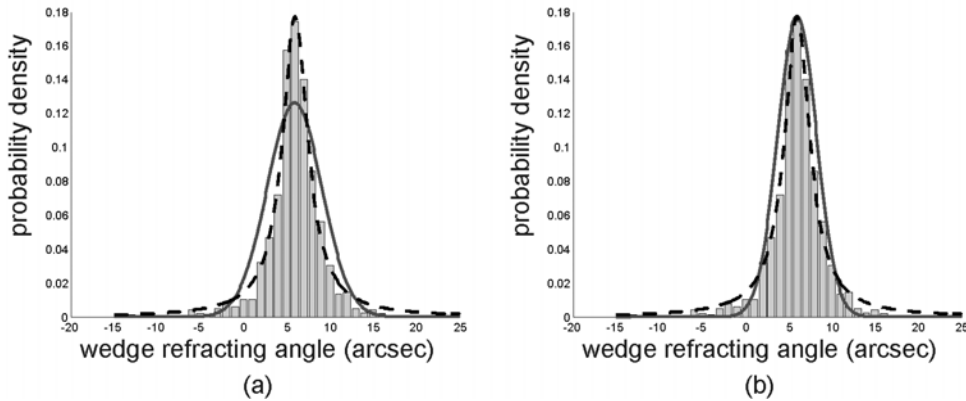


Fig. 6. Probability density function of the wedge refracting angle from the experiment. The parameter $T=1.1$. Broken line - the Cauchy-Lorentz distribution ($x_0 = 5.99$, $\gamma = 1.8$), solid line - the Gaussian distribution - $N(\mu, \sigma^2)$. (a) $N(5.99, 3.1)$ - the calculated parameters μ and σ^2 , (b) $N(5.99, 2.25)$ - the matched parameters μ and σ^2 .

5. Conclusions

This paper presents a precise analysis of data handling error in a new measurement method. A new kind of interferometer OVI is used for small-angle rotation measurement. In the described method the knowledge of the small-angle rotation of the inspected wave allows the calculation of the wedge refracting angle. During calculation the parameter which eliminates one kind of the triplets created by collinear points has been used. Improper choice of these parameters results in a nonsymmetric distribution of the probability density function and subsequently in incorrect measured values of the investigated objects. In this paper the authors present a different way of defining parameters to be used for calculations. Moreover, this paper shows that the result of measurement of the wedge refracting angle with the Optical Vortex Interferometer should be described by the Cauchy-Lorentz distribution. The standard deviation is bigger than the scale parameter specifying the half-width at half-maximum of the Cauchy-Lorentz distribution. In the selected case the value of the standard deviation is 3.1 arcsec and the value of $\gamma = 1.8$ arcsec. The standard deviation used for describing the accuracy of the measurement is misleading.

Acknowledgments

We acknowledge support of this work by the Foundation for Polish Science.

References

- [1] J. Masajada: "Small-angle rotation measurement using optical vortex interferometer". *Opt. Comm.* 239, 2004, pp. 373-381.
- [2] J. Masajada, B. Dubik: "Optical vortex generation by three plane wave interference". *Opt. Comm.* 198, 2001, pp. 21-27.
- [3] L. Allen, S.M. Barnett, M.J. Padgett: *Optical Angular Momentum*. Institute of Physics Publishing, London, 2003.

- [4] J.H. Lee, G. Foo, E.G. Johnson, G.A. Swartzlander Jr: *Experimental Verification of an Optical Vortex Coronagraph*, PRL, 97, 2006, 053901.
- [5] E.G. Johnson, J. Stack, CH. Koehler: "Light Coupling by a Vortex Lens into Graded Index Fiber". *Journal of Lightwave Technology*, vol. 19, no.5, May 2001.
- [6] W. Moa, Y. Zhong, J. Dong, H. Wang: "Crystallography of two-dimensional photonic lattices formed by holography of three noncoplanar beams". *J. Opt. Soc. Am. B.*, vol. 22, no. 5, 2005, pp. 1085-1091.
- [7] W. Wang, N. Ishii, S.G. Hanson, Y. Miyamoto, M. Takeda: "Phase singularities in analytic signal of white-light speckle pattern with application to micro-displacement measurement". *Opt. Comm.* 248, 2005, pp. 59-68.
- [8] A. Popiołek-Masajada, M. Borwińska, W. Frączek: "Testing a new method for small-angle rotation measurements with the optical vortex interferometer". *Meas. Sci. Techno*, no. 17, 2006, pp. 653-658.
- [9] J. Masajada, A. Popiołek-Masajada, D.M. Wieliczka: "The interferometric system using optical vortices as phase marks". *Opt. Comm.* 207, 2002, pp. 85-93.
- [10] J. Masajada, A. Popiołek-Masajada, E. Frączek, W. Frączek: "Vortex point localization problem in optical vortices interferometry". *Opt. Comm.* 234, 2004, pp. 23-28.